Supplement of The Cryosphere, 16, 4659–4677, 2022
https://doi.org/10.5194/tc-16-4659-2022-supplement


The Cryosphere Open Access EGU

*Supplement of*

# New insights into the decadal variability in glacier volume of a tropical ice cap, Antisana (0°29′ S, 78°09′ W), explained by the morpho-topographic and climatic context

**Rubén Basantes-Serrano et al.**

*Correspondence to:* Rubén Basantes-Serrano (ruben.basantes@ikiam.edu.ec)

**SUPPLEMENTARY MATERIAL**

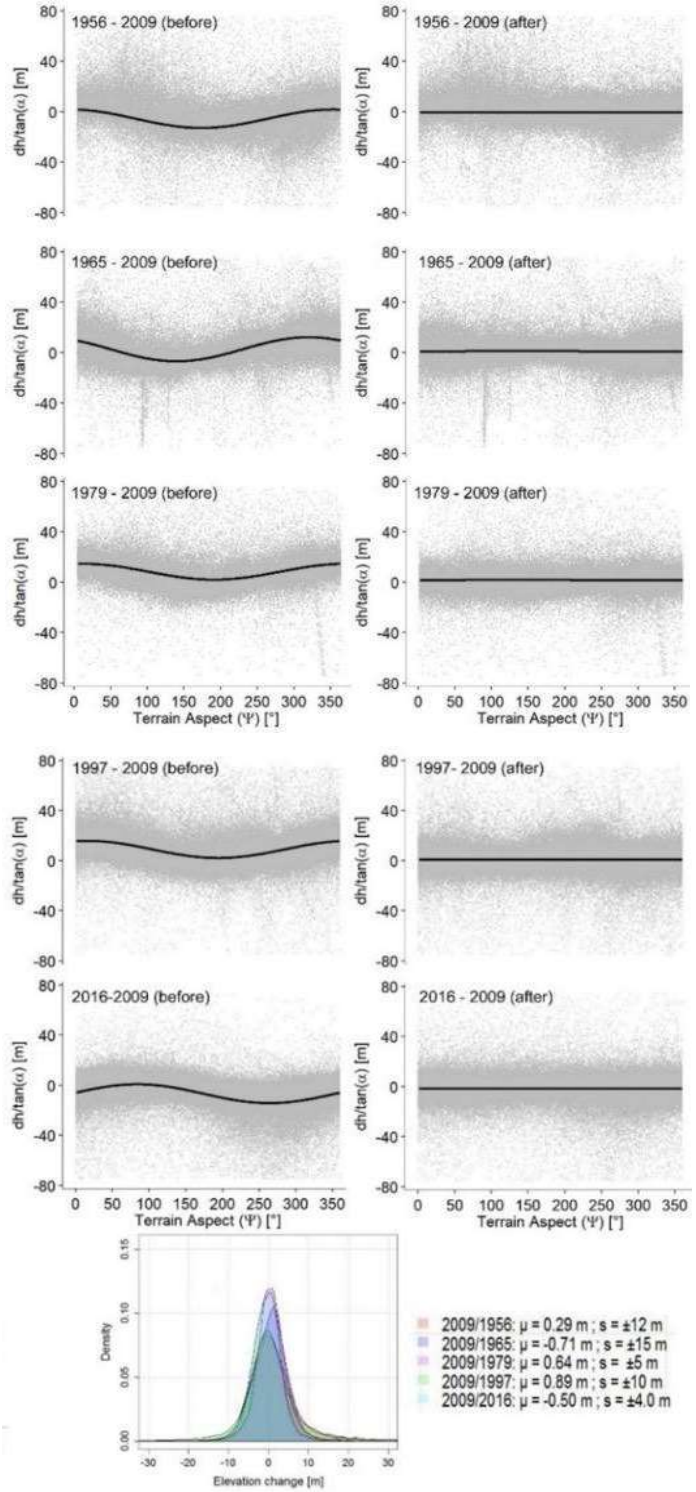


**Fig S1.** Comparison of the standardized elevation for each pixel (grey dots) by the tangent of the slope, as a function of the surface of the ground in the stable rocky areas in the vicinity of the ice cap, before and after co-registration, and the fitted cosine curve (black line). The resulting histograms of the residuals after adjustment for bias.

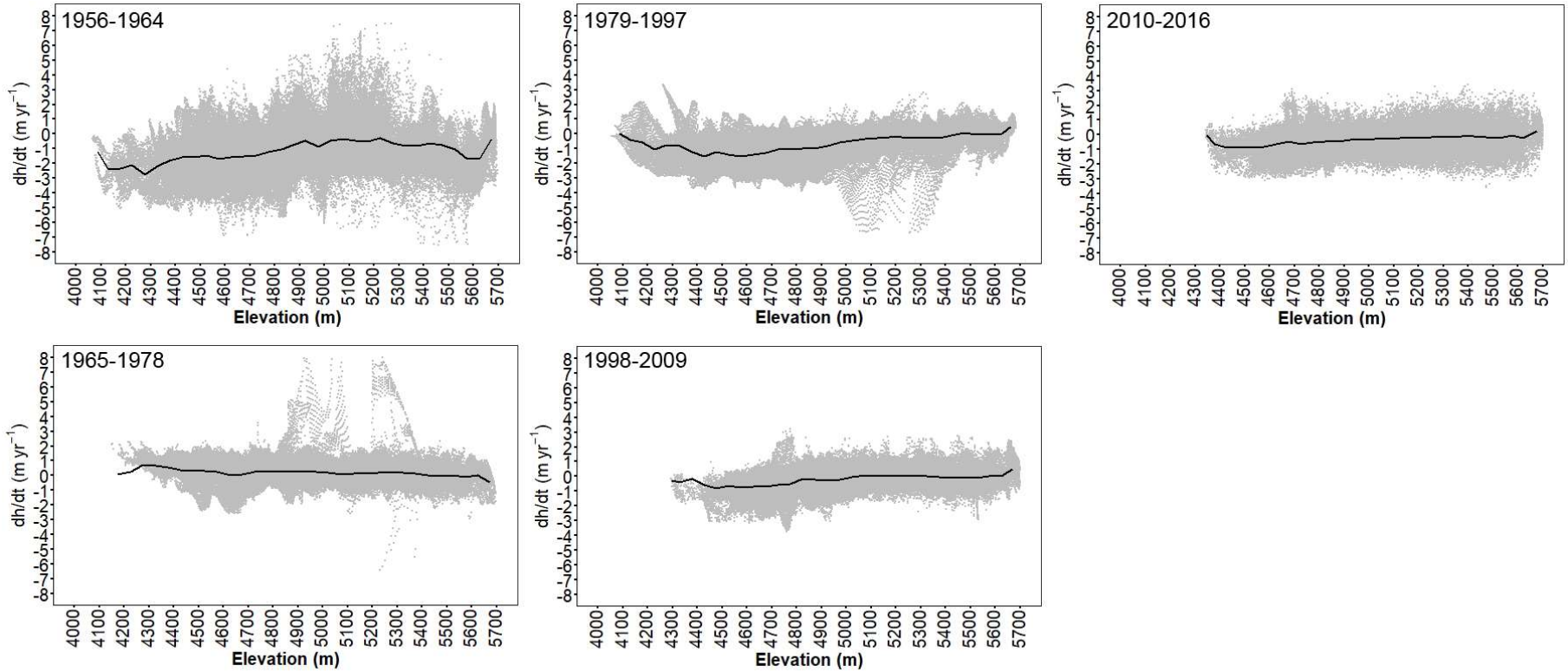


**Fig S2.** The elevation change versus elevation for all the studied periods. One can see that the *dh*-sample point are evenly distributed across the glacier hypsometry.

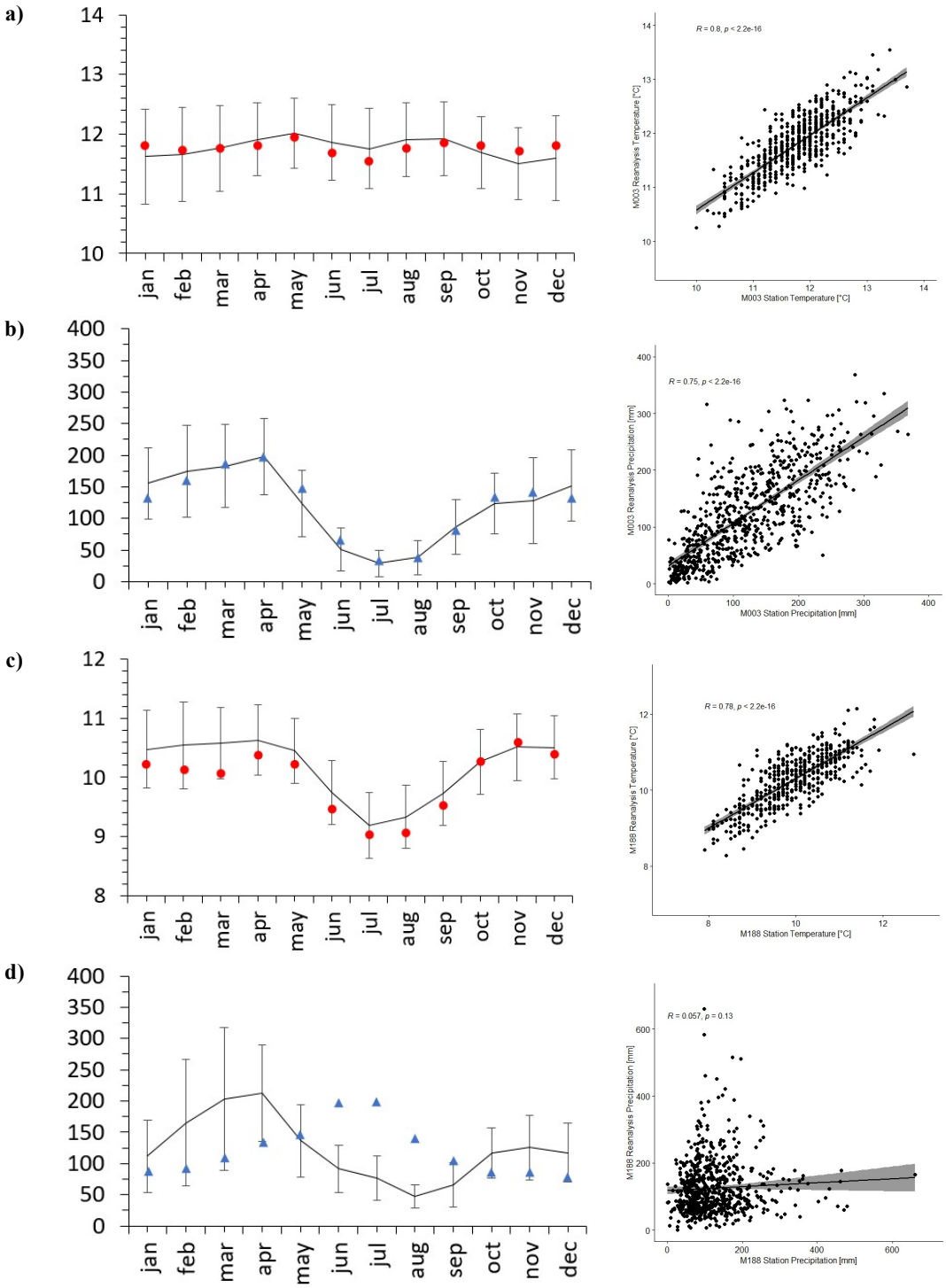


**Fig S3.** Monthly temperature (red circles) and precipitation (blue triangles) and corresponding correlation between stations M003 (a and b)/M188 (c and d) and ERA5 reanalysis data (0.25° × 0.25°) (black line) for the study period. ±1 standard deviations is shown for the grid point nearest to the stations.

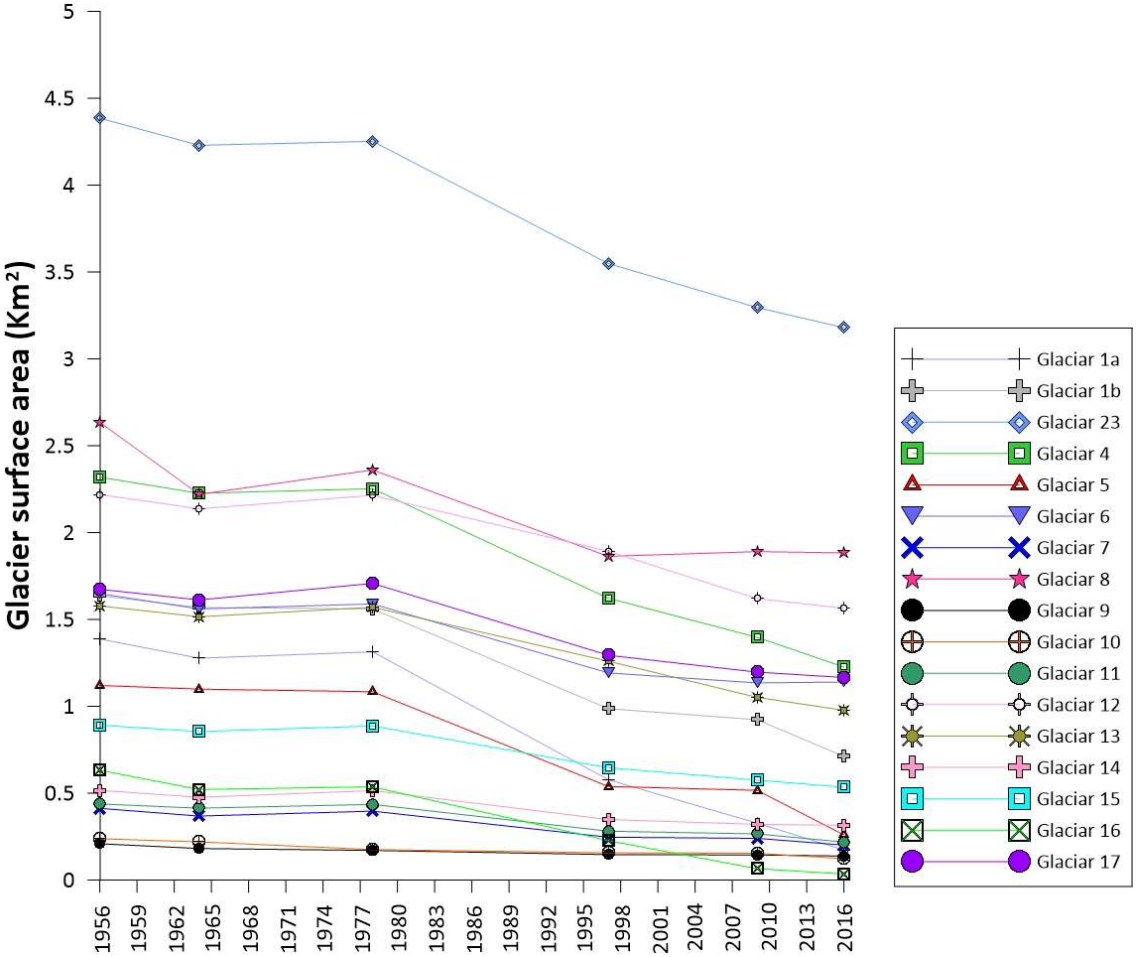


**Fig S4.** Compilation of surface area changes of the 17 glaciers on the Antisana ice cap since the 1956 to 2016.

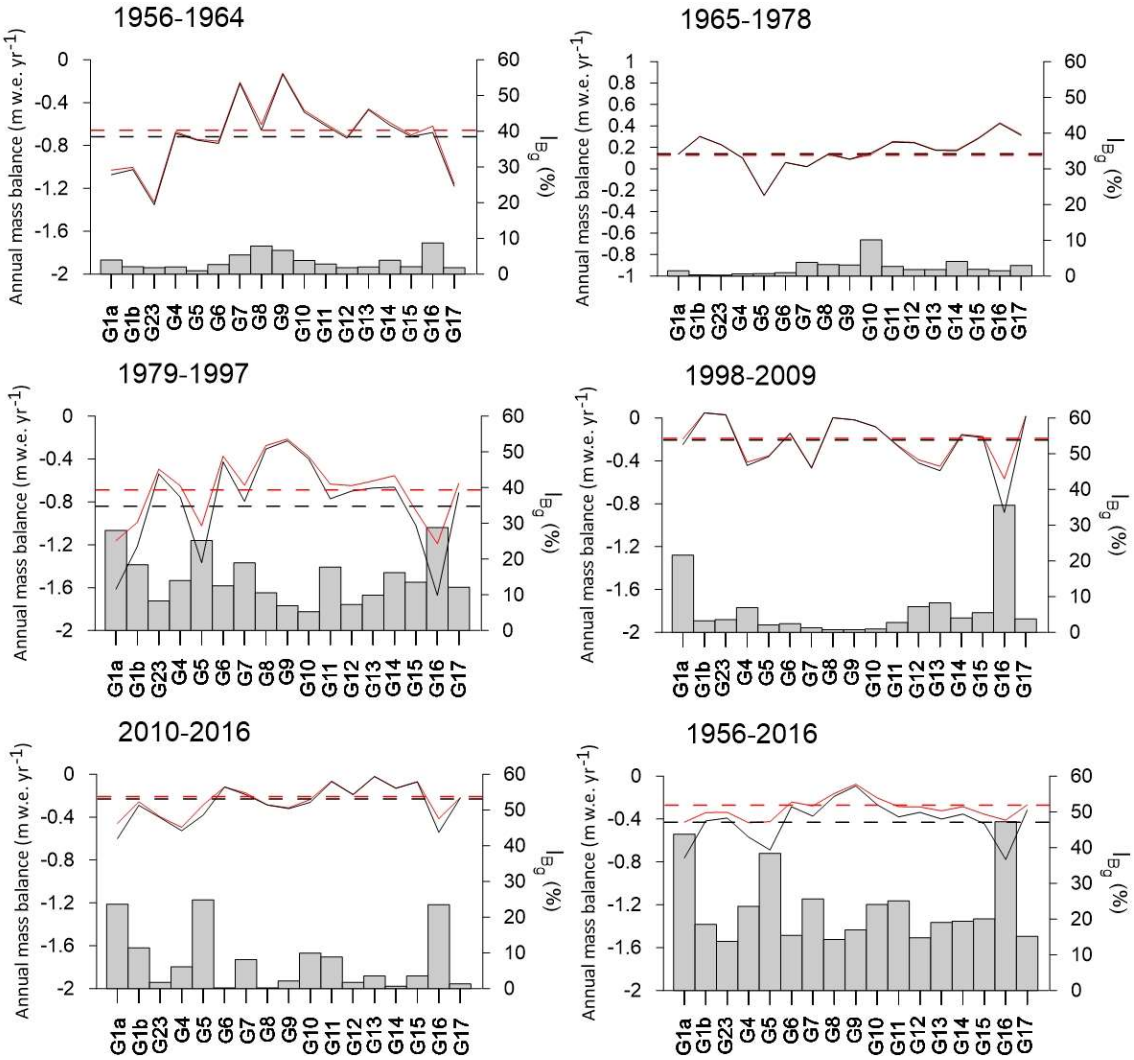


**Fig S5.** Annual glacier mass balance of 17 glaciers on the Antisana ice cap. Glacier-wide balance (solid black line), glacier-wide fixed balance (solid red line), and average annual mass balance (dashed line) for the sub-periods. The right vertical axes show the fraction of the balance on individual glaciers affected if the mean surface-area change is not taken into consideration.

**Table S1.** Characteristics of Antisana glaciers in the 1956-2016 period: Surface area in 2016 ($S_{2016}$), change in surface area ($\Delta S$), maximum altitude ($h_{max}$), mean altitude ($h_{mean}$), median altitude ($h_{medi}$), minimum altitude ($h_{min}$), mean slope ($\alpha$), azimuth ($\phi_{360°}$), orientation ($\phi_{sec}$).

| Name of the glacier | Code | $S_{2016}$ [km$^2$] | $\Delta S_{1956/2016}$ [%] | $h_{max}$ [m a.s.l] | $h_{mean1956/2016}$ [m a.s.l] | $h_{medi1956/2016}$ [m a.s.l] | $h_{min1956/2016}$ [m a.s.l] | $\alpha_{2016}$ [°] | $\phi_{360°}$ | $\phi_{sec}$ |
|---|---|---|---|---|---|---|---|---|---|---|
| **(α)** | G1a | 0.17±0,03 | 88 | 5218 | 4773 / 4982 | 4758 / 4982 | 4435 / 4800 | 28 | 14 | NE |
| **(β)** | G1b | 0.71±0,03 | 57 | 5611 | 4887 / 5034 | 4848 / 4962 | 4325 / 4550 | 32 | 52 | NE |
| **-** | G2,3 | 3.17±0,03 | 28 | 5678 | 4908 / 5039 | 4871 / 5033 | 4067 / 4367 | 29 | 54 | NE |
| **-** | G4 | 1.22±0,02 | 47 | 5582 | 4742 / 4772 | 4699 / 4723 | 4342 / 4434 | 27 | 75 | E |
| **-** | G5 | 0.26±0,02 | 77 | 5070 | 4688 / 4791 | 4676 / 4792 | 4398 / 4671 | 31 | 130 | SE |
| **Azufral** | G6 | 1.14±0,02 | 31 | 5605 | 4870 / 4838 | 4875 / 4761 | 4197 / 4462 | 32 | 148 | SE |
| **-** | G7 | 0.20±0,01 | 51 | 5238 | 4800 / 4900 | 4804 / 4899 | 4480 / 4640 | 37 | 169 | S |
| **De la Caldera** | G8 | 1.88±0,03 | 29 | 5640 | 4990 / 5090 | 4997 / 5060 | 4295 / 4606 | 32 | 181 | S |
| **Cimarrones Oriental** | G9 | 0.14±0,01 | 31 | 5420 | 5034 / 5076 | 5025 / 5079 | 4714 / 4801 | 39 | 190 | S |
| **Cimarrones Central** | G10 | 0.18±0,01 | 21 | 5522 | 5004 / 5046 | 4934 / 4983 | 4649 / 4668 | 40 | 219 | SO |
| **Cimarrones Occidental** | G11 | 0.23±0,01 | 47 | 5538 | 5008 / 5077 | 4911 / 4964 | 4682 / 4668 | 37 | 249 | SO |
| **Great West Los Crespos** | G12 | 1.56±0,03 | 30 | 5698 | 5067 / 5149 | 5008 / 5121 | 4658 / 4718 | 28 | 254 | SO |
| **Los Crespos** | G13 | 0.98±0,02 | 38 | 5703 | 5091 / 5204 | 5017 / 5157 | 4778 / 4845 | 29 | 266 | O |
| **Guagraialina or Los Crespos Norte** | G14 | 0.32±0,01 | 39 | 5469 | 5013 / 5093 | 4979 / 5064 | 4704 / 4830 | 28 | 291 | O |
| **(α, β)** | G15 | 0.53±0,01 | 40 | 5688 | 5106 / 5226 | 5048 / 5211 | 4776 / 4855 | 31 | 313 | NO |
| **-** | G16 | 0.03±0,01 | 95 | 5299 | 4931 / 5121 | 4906 / 5127 | 4750 / 4965 | 32 | 330 | NO |
| **-** | G17 | 1.16±0,02 | 30 | 5697 | 5067 / 5210 | 5007 / 5267 | 4467 / 4645 | 26 | 356 | N |

**Section S1. Comparison with previous estimates of elevation change**

To evaluate the agreement between the elevation changes observed in this study and previous geodetic estimates from Dussaillant et al., (2019), we select a portion of 9 km2, in the western side of the ice cap. See the Randolph Glacier Inventory (RGI) v6.0 for more details. This location was selected because of the limited number of data voids in both datasets (Table S2).

**Table S2.** Average elevation change and percentage of surface area covered by dh-samples.

| Dussaillant et al., (2019) | Data coverage (%) | This study | Data coverage (%) |
|---|---|---|---|
| -0.95 m $a^{-1}$ (2000-2009) | 75 | -0.28±0.06 m $a^{-1}$ (1998-2009) | 85 |
| -0.07 m $a^{-1}$ (2009-2018) | 65 | -0.17 m $a^{-1}$±0.06 (2009-2016) | 84 |
| -0.28 m $a^{-1}$ (2000-2018) | 99 | -0.25 m $a^{-1}$±0.06 (1998-2016) | 99 |

For the full period (1998-2018) we found a good agreement in the elevation change rates, which is not the case for the sub-periods (1998-2009) and (2009-2018) where a noticeable discrepancy is observed (Fig S6). Unlike 1998-2018 period, the dh/ht maps obtained by ASTER imagery tend to be noisy during short peri
ods when the data gaps are around 30%. Data gaps may be related to the presence of cloud or snow cover that prevent the determination of reliable elevation changes. These issues have been previously reported over large Patagonian ice fields (Dussaillant et al., 2019), and could also be the case for a region as humid as the inner tropics where Antisana ice cap is located. However, in spite of the difference observed in ASTERIX data, they are able to capture the similar trend of elevation change rate obtained by this study.

Negative conditions observed in Dussaillant et al., (2019) for the 2000-2009 period are suspicious and does not match with the conditions observed on Antisana glaciers in a similar period (1998-2009), this period has a 25% of data voids resulting in an underestimation of the mass losses.

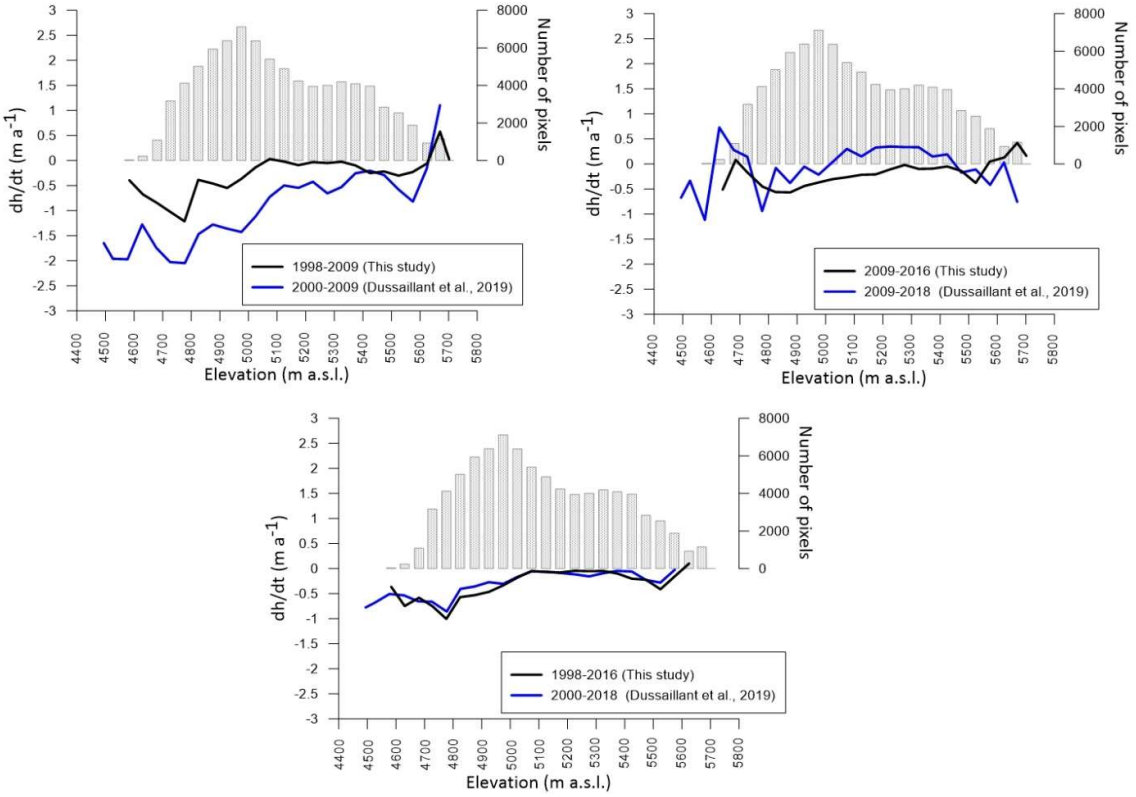


**Fig S6.** The elevation change rate or the western portion of the ice cap (referring as RGI60-16.01339 in the Randolph Glacier Inventory (RGI) v6.0) for the 1998-2018 period and the 1998-2009 and 2009-2018 sub-periods. The glacier hypsometry correspond to the surface area in 1998.

.

**Section S2. Seasonal climate conditions during key periods**

Figure S7 shows no clear relationship between temperature and precipitation anomalies whatever the sub-period considered, but particular features can nevertheless be underlined. We can confirm that cold conditions prevailed until the late 1970s. Warm periods appear to have been enhanced after the beginning of 1980s and have lasted longer in the last decade. Regarding precipitation, the most marked temporal variability occurred in the 1965-1978 and 1979-1997 periods, in which extremely positive or negative mass balances were observed, variability then decreased markedly in the two last decades. It is worth recalling that decadal mass balance variability matches the positive and negative anomalies observed in the Pacific Ocean.

Finally, we stress that in the two key quarters (MAM and SON), 27% of the years can be considered as anomalous, but the quarters differed from one year to the other. Conditions were very cold during the MAM quarter in 10 of the years, and 70% of the cold periods were characterised by humid conditions. During the SON quarter, conditions were more scattered with very cold conditions in 11 of the years during the 1950-1980 period, and with humid conditions in 55% of the years. In the MAM quarter, the strongest "El Niño" events occurred in 1998 (2015/2016) in a wet (dry) context, respectively, while the "La Niña" event of 1999/2000 changed from very wet-cold to dry-cold conditions.

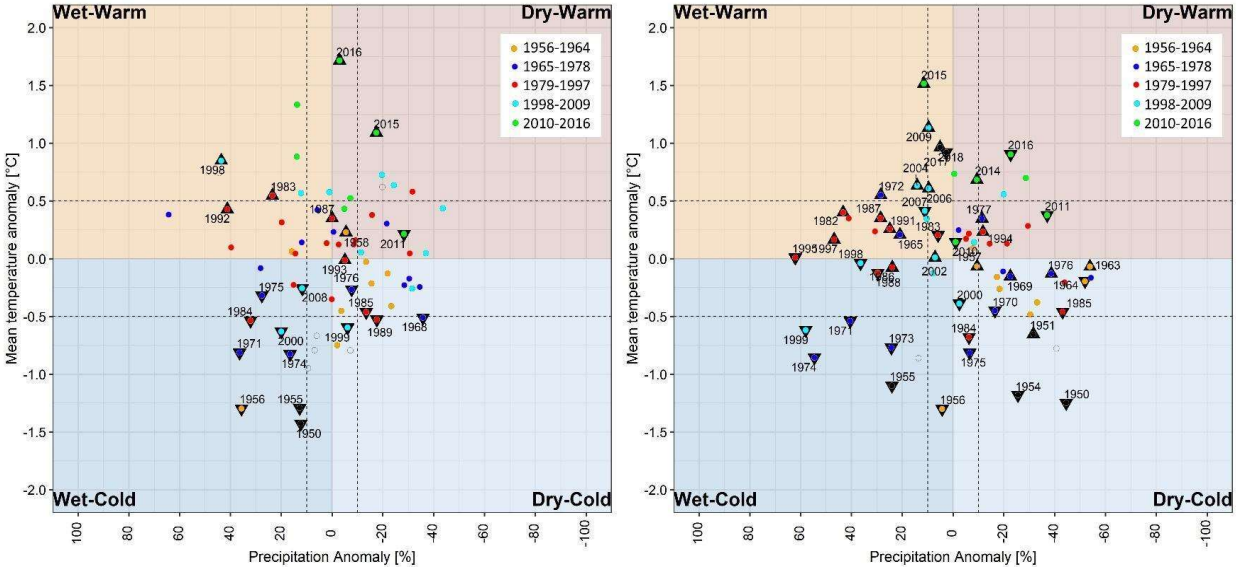


**Fig S7.** Scatterplot of MAM (right) and SON (left) showing temperature and precipitation anomalies in ERA data for the period 1950-2018. The dashed lines show climatic threshold values. Coloured dots represent the centred mass balance for the five sub-periods and the empty circles indicate years with no mass balance. Positive/negative years observed in the Pacific Ocean are indicated by upright/inverted triangles.

Two contrasting situations can thus be highlighted. On the one hand, in a wet-cold context during the MAM quarter, solid precipitation is expected to cover the surface of the glaciers and to remain in place until the following SON quarter, combined with continuous cloudiness, which can reduce the effects of incoming solar radiation, thereby weakening ablation. This situation may be accentuated during the cold “La Niña” events. On the other hand, if precipitation is scarce and/or liquid during warm periods, combined with less cloud cover, incoming solar radiation will enhance ablation by increasing ice melt during the equinoxes. In fact, at the scale of the Antisana ice cap, the glaciers’ response is in good agreement with the cold/warm periods illustrated by the Southern Oscillation Index (SOI). At a sub-decadal time step, *in-situ* observations revealed a strong influence of ENSO episodes on glacier response, in this context, it is reasonable to assume a cumulative effect of ENSO events at multi-decadal scale.